Preprints of the 19th World Congress
The International Federation of Automatic Control
Cape Town, South Africa. August 24-29, 2014

Multiple-Disturbance Rejection for High Precision Positioning of a VCM Servo Gantry ⋆

Zeshan Lyu * **Peng Yan** *,**,1 **Zhen Zhang** *** **Lei Guo** *

* *School of Automation Science and Electrical Engineering, Beihang University, Beijing, 100191, China.*
** *Key Laboratory of High-efficiency and Clean Mechanical Manufacturing, Ministry of Education, School of Mechanical Engineering, Shandong University, Jinan, Shandong, 250061, China.*
*** *Beijing Key Lab of Precision/Ultra-Precision Manufacturing Equipment and Control,Department of Mechanical Engineering, Tsinghua University, Beijing 100084, China.*

Abstract: This paper presents an multiple disturbance rejection approach for rejecting narrow-band disturbances as well as norm-bounded random disturbances, with applications to high precision positioning of a Voice Coil Motor (VCM) actuated servo stage. An adaptive optimal phase filter design method is proposed for the rejection of frequency-varying narrow-band disturbances at unknown frequency range. With a parallel connection of the proposed adaptive filter, a robust H_∞ controller can be synthesized with mixed sensitivity optimization for the purpose of both robust stability and rejection of norm-bounded random disturbances. The proposed control architecture is implemented to a VCM servo gantry to achieve high precision positioning in the presence of various disturbances.

Keywords: Mechatronics, Disturbance Rejection, Adaptive Filter, Robust Control.

1. INTRODUCTION

Disturbance rejection is one of the key challenges in high precision control of mechatronic systems. The problem is particularly critical when multiple sources of disturbances exist, such as disk shifts and spindle vibrations in hard disk drive system (see Sri-Jayantha (2001)), current and voltage harmonics interference in power systems with nonlinear loads (see Routray *et al*. (2001)) and torque disturbance in the actuators for the target positioning (see Shibasaki *et al*. (2013)).The positioning and tracking accuracy of advanced servo systems require disturbances rejection on narrow band noises as well as broad band noises. Accurately, the disturbance discussed here mainly refers to broad-band Gaussian noises at relative low frequency band and narrow-band disturbance with unknown center frequency.

Much progress has been made in the field of disturbance rejection, expecially attracting both academic research and industry implementations. For example, proportional-integral-derivative (PID) controller design is popular for its simplicity in design process (see Han (2010)). In addition, Chen *et. al* put forward the adaptive back stepping fuzzy control approach to reject the periodic disturbances (see Chen *et al*. (2010)). However, the tuning of PID controller or fuzzy controller is mostly determined by rule of experience, which will lead to the influence of overshot (see Han (2010)). Note that for the narrow-band disturbance rejection, existing results on filter designs can only be used to reject narrow-band disturbances at specific limited frequency band, such as the peak filter in low-frequency band, phase-lead peak filter in the mid-frequency band and phase-stabilized servo controller in high-frequency band (see Zheng *et al*. (2006)). More recently Zheng *et. al* introduces a second-order generalized disturbance filter to effectively suppress narrow-band disturbances at any unlimited frequency range. However, the existing frequency band of narrow-band disturbances should be known in advance in the filter design, which limits its practical implementation because the frequency of narrow band disturbance could probably be unknown in time-varying ranges. It is desirable to develop an adaptive generalized disturbance filter whose coefficients are determined by error information and time series (see Chen *et al*. (2012)).

Sinusoidal signal frequency detection and elimination is a classical problem with many practical applications (see Mojiri *et al*. (2004), Pyrkin *et al*. (2012), Pigg *et al*. (2010), Aranovskiy *et al*. (2010)). Some industrial methods and well-studied control methods have been developed recently for this purpose, such as phase lock method, seeker optimization algorithm (see Dai *et al*. (2010)), online estimator based on plant parameterizations (see levin *et al*. (2011)) with adaptive scheme, predictor feedback approach with low adaptive scheme (see Guo *et al*. (2012)) and adaptive notch filtering(see Regalia (2010), Took *et al*. (2010)). However, The performance of the above methods could often be either effected by the modeling dynamics or the relative high dimensions of the adaptive coefficients. It is worth mentioning that Ferdjallah *et. al* proposed an adaptive digital notch filter design on the unit circle by combining LMS algorithm and IIR or FIR filter (see Ferdjallah *et al*. (1994)). In the present paper, similar idea will be employed to

⋆ We would like to thank the financial support from the NSFC (grant No. 61327003 and 61004004), China Fundamental Research Funds for the Central Universities under Grant No. 10062013YWF13-ZY-68, Tsinghua University Initiative Scientific Research Program (grant no. 2010Z02270) and Specialized Research Fund for the Doctoral Program of Higher Education (grant no. 20100002120043).

[1] All correspondence should be addressed to: Peng Yan (email: PengYan2007@gmail.com).

investigate the adaptive filter design, where convergence analysis is also provided.

The main contribution of the present work is the development of an adaptive disturbance filter with the nature of optimal phase such that it can be combined with robust controller synthesis. The overall robust control structure is capable of rejecting both time varying narrow band disturbances, as well as norm-bounded broad band disturbances. The proposed control architecture can be well implemented to the servo positioning of mechatronic systems.

The rest of the paper is organized as follows. Some preliminary results on optimal phase filter is discussed in section 2. An adaptive optimal phase filter design method is proposed and analyzed in section 3, followed by the synthesis of robust H_∞ controller in section 4. Simulations and real time experiments are provided in section 5 to demonstrate the high precision positioning of this control architecture and some concluding remarks are given in section 6.

2. PRELIMINARIES ON OPTIMAL PHASE FILTER

We first recall the generalized second order disturbance filter for suppression of narrow-band disturbances (see Zheng *et al.* (2006)). Different from other notch filters, the numerator of the generalized disturbance filter is embedded with an optimal phase angle φ, which is determined by the complex phase of the complementary sensitivity function $T(s)$ of closed-loop system at the disturbance center frequency ω_0. The optimal phase notch filter can be written as:

$$F(s) = K\frac{s[\omega_0 cos(\varphi) - \sin(\varphi)s]}{s^2 + 2\zeta\omega_0 s + \omega_0^2}, \tag{1}$$

where ω_0 is the center frequency of the narrow band disturbance, φ is the optimal phase angle being determined by φ=arg$[T(j\omega_0)]\in[-\pi,\pi]$, $\zeta\in(0,1)$ is the damping ratio and $K>0$ is the filter gain.

As depicted in Fig. 1, when the switch is off, we denote the sensitivity function and complementary sensitivity function of the model plant $P(s)$ and controller $C(s)$ as

$$S_0(s) = \frac{1}{1+P(s)C(s)} \quad T(s) = \frac{P(s)C(s)}{1+P(s)C(s)} \tag{2}$$

When the switch is on, we can denote the new sensitivity function of the closed loop as

$$\begin{aligned} S(s) &= \frac{1}{1+PC(1+F)} \\ &= \frac{1}{1+PC}\cdot\frac{1+PC}{1+PC+PCF} = S_0(s)\cdot S_F(s) \end{aligned} \tag{3}$$

Recall the analysis presented, we have the following observations:

1.1) Thanks to the decoupling of sensitivity functions, the optimal phase filter can achieve a adjustable gain attenuation at a narrow frequency band centered at ω_0, where the attenuation gain can be determined by

$$|S_F(j\omega_0)| = \frac{1}{|1+T(j\omega_0)F(j\omega_0)|} \geq \frac{1}{1+|T(j\omega_0)||F(j\omega_0)|} \tag{4}$$

and its minimum value can be estimated by

$$\arg[T(j\omega_0)] + \arg[F(j\omega_0)] = 0; \tag{5}$$

1.2) The sensitivity loop gains at all other frequencies (except ω_0) will be similar for S_0 and S(in Fig. 2).

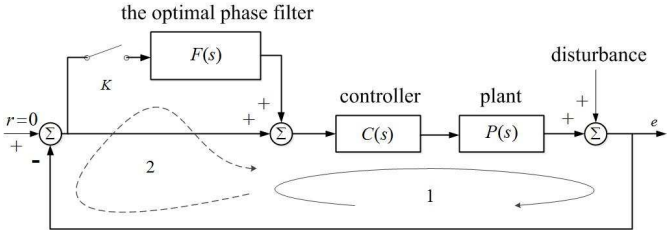

Fig. 1. Block diagram of a parallel control structure with the optimal phase filter.

3. ADAPTIVE DIGITAL OPTIMAL PHASE FILTER

A ω_0-fixed optimal phase filter may eliminate the narrow-band disturbance when the distribution is centered exactly at the disturbance frequency ω_0. However, if the disturbance distribution is not centered at the disturbance frequency ω_0, for instance ,varying around a specific frequency or from one frequency to another one, the ω_0-fixed optimal phase filter may be ineffective[5], which makes an adaptive optimal phase filter necessary. In the past researches, adaptive algorithms are commonly applied in several kinds of filters and controller design, such as Adaptive notch filer design in Regalia (2010). LMS algorithm has been widely applied into several applications and especially to reject the Gaussian noise in the desired input signal such as. The transfer function of optimal phase filter can be derived after discretion as (signal sample frequency ω_s, sampling interval T_s=$2\pi/\omega_s$)

$$F(z) = \frac{b_0 + b_1 z^{-1} + b_2 z^{-2}}{1 + a_1 z^{-1} + a_2 z^{-2}} \tag{6}$$

we notice that the denominators of optimal phase filter transfer function are the same with that of a second-order IIR notch filter, the denominator coefficients of optimal phase filter are determined as follows

$$a_1 = -2\alpha\cos(\omega_0 T), a_2 = \alpha^2 \tag{7}$$

Where $\alpha\leq 1$ to guarantee the optimal phase filter stability and (1-α) is the distance between the poles and zeroes of a second-order IIR notch filter (see Ferdjallah *et al.* (1994)). As the disturbance frequency (rejected frequency) ω_0 varies away from or around nominal noise frequency, there is only one filter coefficient a_1 to be adapted to track the disturbance frequency variation under certain allowed error condition, for that the change of φ effects little on the attenuation in the sensitivity curve,as depicted in Fig. 2.

For single coefficient adaptation, we optimize the block diagram in Fig. 1 to Fig. 3 by utilizing the error signal in the filter design and regard minimizing the error signal as the adaptive purpose. As shown in Fig. 3, an adaptive optimal phase filter consists of outside input signal $r(t)$, filter input signal $x_1(t)$, filter output signal $y_1(t)$, controller input signal $x_2(t)$, plant output signal $y_2(t)$, error signal $e(t)$ and disturbance signal $d(t)$,including narrow-band disturbance signal $d_1(t)$ and noise signal $d_2(t)$. In the experiment and simulation, we consider $r(t)$=0 by default and make the narrow-band disturbance the only signal source for the whole system. In the first section of the block diagram, we suppose that the input signal number comes to n, we regard $x_1(n)$ as the input signal for the adaptive optimal phase filter and $y_1(n)$ as the filter output signal, filter coefficient $a_1(n)$ as the value of a_1 at this moment. The adaptive optimal phase filter gives that

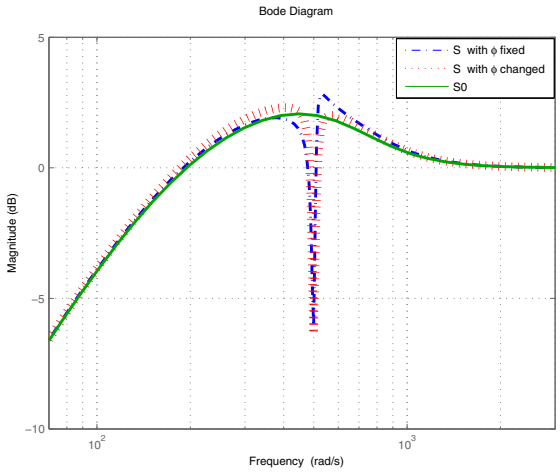

Fig. 2. Effects of φ on the sensitivity curve $S(s)$.

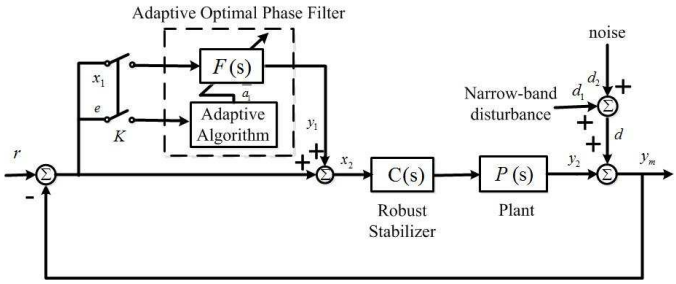

Fig. 3. Block diagram of the adaptive optimal phase filter.

$$F(z)=\frac{b_0+b_1z^{-1}+b_2z^{-2}}{1+a_1(n)z^{-1}+a_2z^{-2}} \tag{8}$$

Then we would like to review the new iteration algorithm derivation in the following parts in this section. To simplify the equation derivation, product of the plant $P(s)$ and the controller $C(s)$ after respective discretization can be determined as

$$C(z)P(z)=\frac{c_0+c_1z^{-1}+\cdots+c_Mz^{-M}}{1+d_1z^{-1}+\cdots+d_Nz^{-N}}(M>N) \tag{9}$$

Coefficients matrixes of $F(z)$ and $C(z)P(z)$ can be deduced as

$$A(n)=[a_1(n)\ a_2\ 0\ \cdots\ 0]_{1\times(M+1)} \tag{10}$$

$$B=[b_0\ b_1\ 0\ \cdots\ 0]_{1\times(M+1)} \tag{11}$$

$$C=[c_0\ c_1\ \cdots\ c_M]_{1\times(M+1)} \tag{12}$$

$$D=[d_1\ \cdots\ d_N\ 0\ \cdots\ 0]_{1\times(M+1)} \tag{13}$$

It is easy to find that the matrix B, C and D are all the time-invariant matrixes, we can also clearly know from the block diagram that

$$y_1(n)=BX_1^T(n)-A(n)Y_1^T(n) \tag{14}$$

$$y_2(n)=CX_2^T(n)-D(n)Y_2^T(n) \tag{15}$$

$$x_2(n)=x_1(n)+y_1(n) \tag{16}$$

Besides, signal state matrixes $X_1(n)$,$Y_1(n)$and $Y_2(n)$ can be determined as

$$X_i(n)=[x_i(n)\ \cdots\ x_i(n-M)]_{1\times(M+1)}(i=1,2) \tag{17}$$

$$Y_i(n)=[y_i(n-1)\ \cdots\ y_i(n-M-1)]_{1\times(M+1)}(i=1,2) \tag{18}$$

$$X_2(n)=X_1(n)+Y_1(n+1) \tag{19}$$

Error signal $e(n)$ and disturbance signal $d(n)$ are connected as follows

$$e(n)=r(n)-d(n)-y_2(n) \tag{20}$$

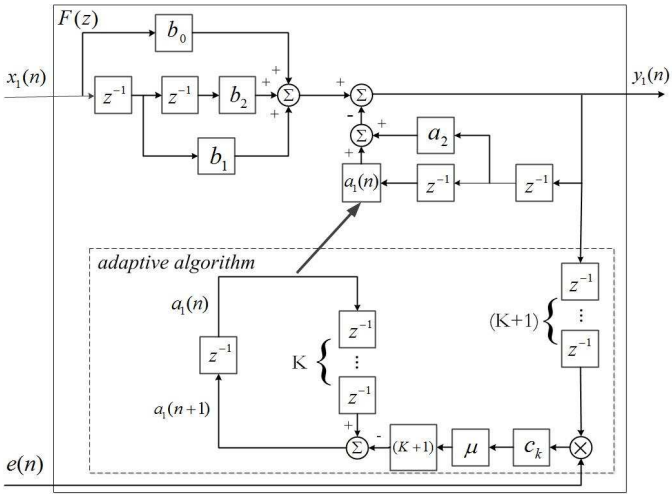

Fig. 4. Digital implementation block diagram of adaptive optimal phase filter.

Generally, the error signal $e(n)$ can be minimized by many recursive algorithms and the most widely used method may be recursive least mean square algorithm. Take the mean square value of error signal as penalty function. In order to minimize the iteration delay and estimate gradient vector with instantaneous value, we can deduce the gradient of $e_1^2(n)$ to the adaptive coefficient $a_1(n-k)$ (where c_k is the first nonzero coefficient when denominator coefficients of $C(z)P(z)$ are sorted by descending power of z)

$$\begin{aligned}\hat{\nabla}J(n)&=\frac{\partial[e^2(n)]}{\partial[\hat{a}_1(n-k)]}=2e(n)\frac{\partial[e(n)]}{\partial[\hat{a}_1(n-k)]}\\&=-2c_ke(n)y_1(n-k-1),0\le k<N\end{aligned} \tag{21}$$

And the iteration equation of adaptive optimal phase filter also needs modification As shown in the Fig. 4, it can easily give that

$$\hat{a}_1(n+1)=\hat{a}_1(n-k)+(k+1)\mu c_ke(n)y_1(n-k-1),0\le k<N \tag{22}$$

When the iteration number comes to $(n+1)$, we can determine the adaptive coefficient $a_1(n+1)$ by the value of $\hat{a}_1(n+1)$ mentioned above. So the coefficient iteration will last for an adaptive time ΔT until the mean square value of error signal converges to a steady minimum and then the adaptive optimal phase filter has tracked and rejected the frequency-unknown narrow-band disturbance. The adaptive time ΔT changes with the value of iteration step μ, which will be discussed in the next sections.

4. ROBUST SERVO POSITIONING WITH MULTIPLE-DISTURBANCE

Besides the narrow-band disturbance discussed in the previous sections, broad band random disturbances with bounded norm also widely exist in mechatronic systems. Therefore, robust stabilizer can be designed to ensure that the sensitivity function curve has optimized performance for system uncertainties and rejection capability for random disturbances bandwidth. We would like to propose a mixed sensitivity H_∞ problem as depicted in Fig. 5 to optimize the robust stabilizer design.

Mixed sensitivity problem aims to optimize a canonical rational function controller to ensure basic stability and performance of the servo system. For the robust control problem depicted in the

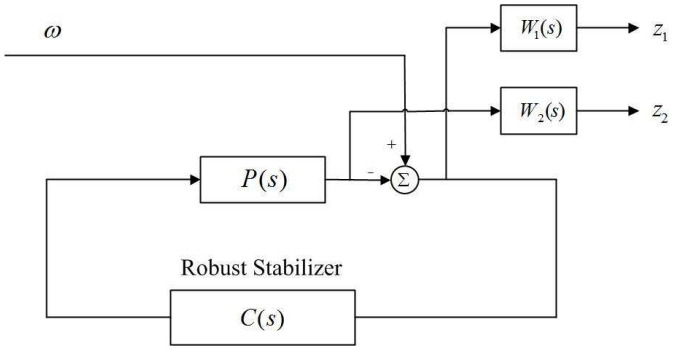

Fig. 5. Structure of mixed sensitivity control.

block diagram of Fig. 3, it is necessary to make compromises about the gains of both $S_0(s)$ and $T(s)$ in the different frequency bands, in the hope of taking into account both the performance of rejecting disturbance and effects of system uncertainties, .

Our design object is to

$$\inf_{Cstab.P} \left\| \begin{bmatrix} W_1(s)S_0(s) \\ W_2(s)T(s) \end{bmatrix} \right\|_\infty \tag{23}$$

where $W_1(s)$ is sensitivity weighting function and $W_2(s)$ is uncertainty weighting function. According to the relative determination methods mentioned in (Doyle *et al*. (1990) and Leng *et al*. (2013)), $W_1(s)$ and $W_2(s)$ can be selected as

$$W_1(s) = \frac{K_1}{(s+\varepsilon)^2} \tag{24}$$

$$W_2(s) = K_2 \frac{s^2 + l_1 s + l_2}{s^2 + m_1 s + m_2} \tag{25}$$

where the coefficients in $W_1(n)$ and $W_2(n)$ can be determined in the experiments, with which the optimal robust stabilizer can be designed (Doyle *et al*. (1990)).

5. SIMULATIONS AND EXPERIMENTS

In this section, the proposed parallel control architecture connection of the adaptive optimal phase filter and robust controller is implemented on a VCM servo gantry for the high precision positioning with the existence of various disturbances.

5.1 System Setup

The multiple-disturbance rejection approach is applied to VCM gantry using real time control execution system of xPCTarget and NI data acquisition hardware. Positioning sensors of VCM actuated servo gantry are linear encoders with resolution of 50 nanometer. The control current to VCM actuators are regulated by linear power amplifiers with bandwidth around 2000Hz. We employ Matlab/Simulink real time control package xPCTarget with NI PCI-6251 I/O hardware for control systems implementations. Sampling frequency is selected as 10KHZ for controls and data acquisitions.

The augmented plant can be determined by frequency response experiments as

$$P(s) = \frac{2.239e4}{s^2 + 131.5s + 84.9} \tag{26}$$

As described above,$W_1(s)$ and $W_2(s)$ can be selected as

$$W_1(s) = \frac{2}{(s+0.1)^2} \tag{27}$$

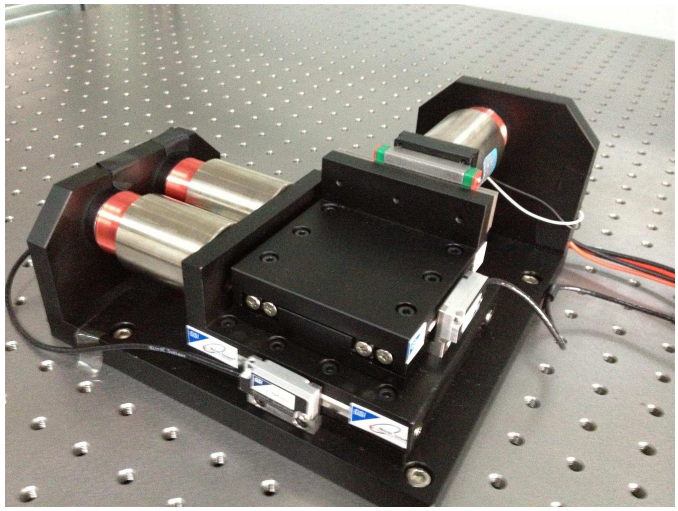

Fig. 6. X-Y voice coil motor servo stage.

$$W_2(s) = 20000 \frac{s^2 + 888.4s + 3.948e5}{s^2 + 8.884e4s + 3.948e9} \tag{28}$$

Therefore, the robust stabilizer can be designed as 6-order.

5.2 Frequency-invariant Disturbance Adaptive Rejection

In the experiment, we select a disturbance signal which consists of a single sinusoidal and Gaussian noise with flat spectral content in low frequency band.

$$\begin{aligned} d(t) &= d_1(t) + d_2(t) \\ &= A_1 \sin(\omega_1 t) + n(t) \end{aligned} \tag{29}$$

The input of the system is selected as zero by default

$$r(t) = 0 \tag{30}$$

To make sure the coefficient adaptation tuning, the sinusoidal frequency ω_1 should be selected different from the initial filter notch center frequency ω_0. The filter parameters are chosen as follows: $\omega_1 = 200rad/s, \omega_0 = 300rad/s, A = 0.1\mu m, T_s = 0.0001s, \mu = 0.1$. When the switch K is turned on and the adaptive optimal phase filter is connected in the system closed-loop, Fig. 7(a) shows the positioning error signal in simulation and experiment on the VCM servo gantry system and Fig. 7(b) shows the adaptive process of coefficient $a_1(n)$. The experimental results show that these parameters are robust for the whole system and the adaptive optimal phase filter shows good performance in tracking and rejecting the invariant-frequency narrow-band disturbances.

The selection of iteration step μ acts as the significant part in the algorithm recursive iteration process. In the simulation result of Fig. 8, iteration step μ chooses different values as $0.05, 0.1, 0.2, 0.5$. Fig. 8 shows effects of the change of iteration step μ on the iteration process, and μ can be selected for the system stability according to Routh Stability Citiration.

5.3 Frequency-varying Disturbance Adaptive Rejection

In experiment 2, we select a disturbance signal which consists of a single sinusoidal whose frequency varies with time series and Gaussian noise with flat spectral content.

$$\begin{aligned} d(t) &= d_1(t) + d_2(t) \\ &= A_1 \sin[\omega_1(t)t] + n(t) \end{aligned} \tag{31}$$

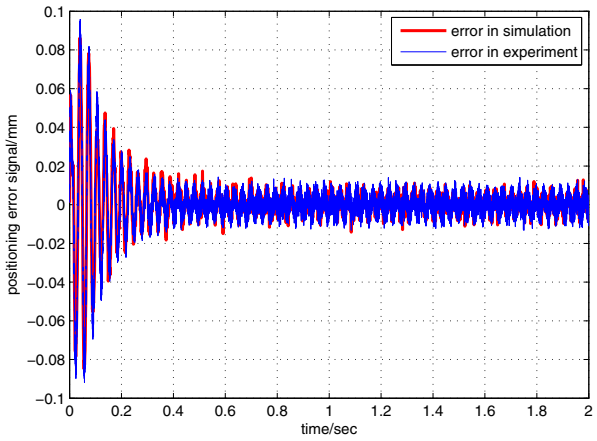

(a) Error signal without and with AOP filter

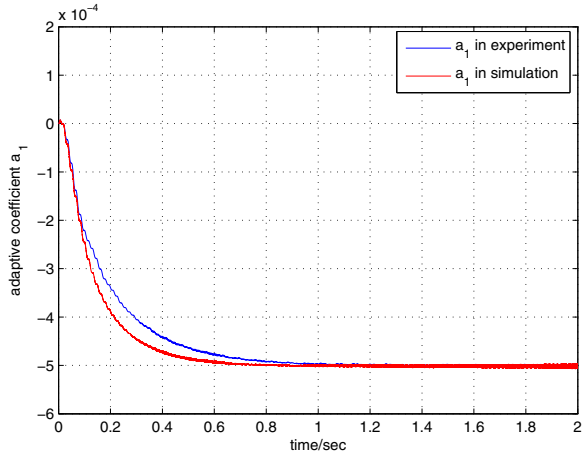

(b) Adaptive process of $a_1(n)$

Fig. 7. Rejection for frequency-invariant sinusoidal with white noise.

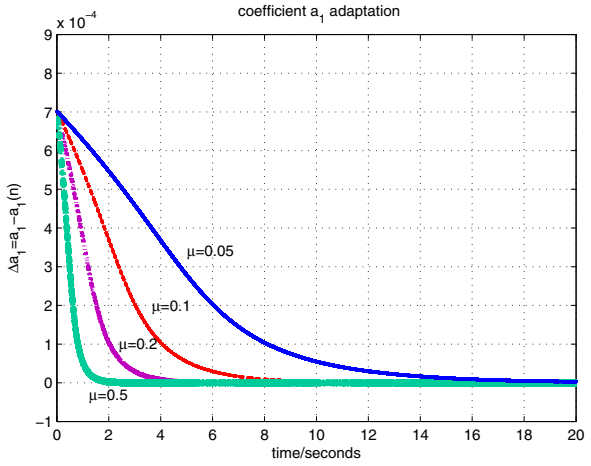

Fig. 8. Effects of the change of iteration step μ on the iteration process

$$\omega_1(t) = \omega_{1,n}, 2N_T\pi\sum_{i=1}^{n}\omega_{1,i} < t < 2N_T\pi\sum_{i=1}^{n+1}\omega_{1,i} \qquad (32)$$

where $1 \le n \le (N+1), i, n, N, N_T \in N^*$

$$\omega_{1,n} = \omega_{1,A} + \frac{n-1}{N}(\omega_{1,B} - \omega_{1,A}) \qquad (33)$$

We consider the disturbance frequency varies with time series. The varying process is as follows: the frequency $\omega_1(t)$ varies from $\omega_{1,A}$ to $\omega_{1,B}$ in a time period of T, for the same reason in experiment 1, the initial sinusoidal frequency $\omega_{1,A}$ should be selected different from the initial filter notch center frequency ω_0 . Every frequency $\omega_{1,n}$ stays stable for N_T time periods at this frequency. The filter parameters are chosen as follows:

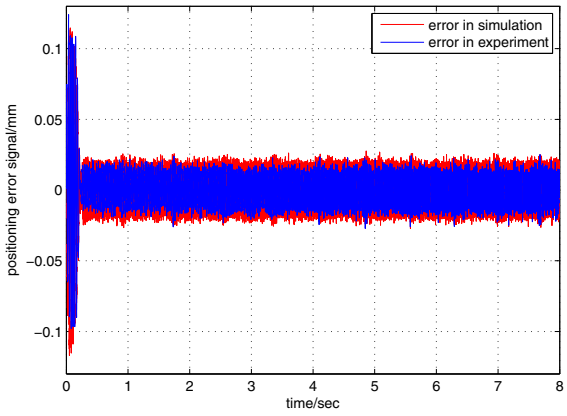

(a) Error signal without and with AOP filter

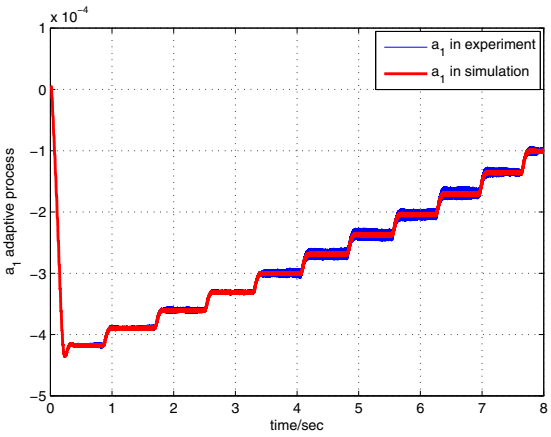

(b) a_1 Adaptive process for time-varying frequency sinusoidal with white noise

Fig. 9. Rejection for time-varying frequency sinusoidal with white noise.

$\omega_{1,A} = 450rad/s$, $\omega_{1,B} = 350rad/s$, $\omega_0 = 300rad/s$, $N_T = 5$, $N = 10$, $A = 0.1\mu m$,$\mu = 2$ in *Simulink* simulations and servo gantry experiments. Fig. 9(a) shows both the simulation and experiment results of the positioning error signal when the Switch K is on. Fig. 9(b) shows the adaptive coefficient change in the adaptive process to track the frequency-varying disturbance in the simulation and experiment. Every time the frequency of narrow-band disturbance changes, the adaptive filter coefficient $a_1(n)$ relatively starts to converges to a new steady value after a short adaptive process. The simulation and experimental results demonstrate that the adaptive optimal phase filter can not only reject the unknown frequency-invariant narrow-band disturbance but also track and suppress the frequency-varying narrow-band disturbances.

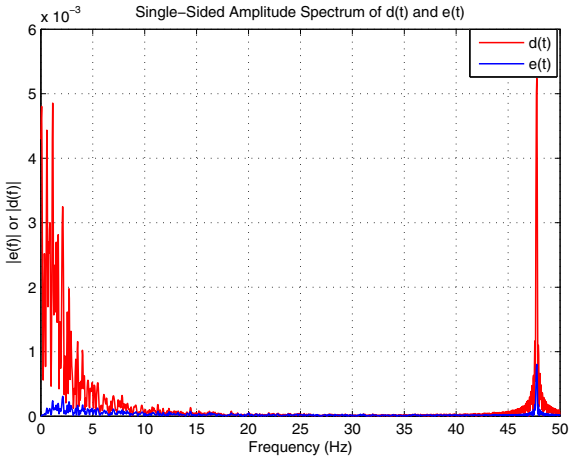

Fig. 10. Multiple-disturbance attenuation in amplitude spectrum

5.4 Multiple-disturbance Rejection Analysis

In the mentioned simulations and experiments, we consider the disturbance to be rejected as some random noise in the relative low frequency band and narrow-band or harmonic signals in the middle or high frequency band. Through the Fast Fourier Transformation(FFT) of the disturbance input signal $d(t)$ and positioning error signal $e(t)$, we can get the information of amplitude spectrum of the two signals in Fig. 10. By the comparison, we can apparently notice the wide amplitude attenuation in low frequency band and approximate attenuation by 84.6% in relatively high frequency narrow-band, which clearly verifies the disturbance rejection performance of the proposed approach.

6. CONCLUSIONS

An adaptive optimal phase filter is developed to suppress time-varying narrow-band disturbances. The convergence and performance of the proposed filter is also discussed. With a parallel connection control structure, we further introduce mixed-sensitivity based robust stabilizer for the purpose of robust stability and random disturbance rejections. The multiple-disturbance rejection approach is applied to a VCM servo gantry system for high precision positioning. Simulations and Experiments demonstrate good performance on the convergence of the adaptive algorithm and the overall performance of rejecting various disturbances.

REFERENCES

S. M. Sri-Jayantha. True track TM servo technology for high TPI disk drives. *IEEE Transaction on Magnetics*, volume 37, number 2, pages 871–876, March, 2001.

A. Routray, A. K. Pradhan and K. P. Rao. A novel kalman filter for frequency estimation of distorted signals in power systems. *IEEE Transactions on Instruments and Measurements*, volume 51, number 3, pages 469–479, June, 2002.

H. Shibasaki, R. Tanaka, H. Ogawa and Y. Ishida. High speed activation and stopping control system using the bang-bang control for a DC motor. *IEEE International Symposium on Industrial Electronics*, Taipei, Taiwan, pages 1–6, May, 2013.

J. Han. From PID to active disturbance rejection control. *IEEE Transactions On Industrial Electronics*, volume 56, number 3, pages 900–906, March, 2009.

W. Chen, L. Jiao, R. Li and J. Li. Adaptive backstepping fuzzy control for nonlinearly parameterized systems with periodic disturbances. *IEEE Transactions on Fuzzy Systems*, volume 18, number 4, pages 675–684, August, 2010.

J. Zheng, G. Guo, Y. Wang and M. Fu. A generalized disturbance filter design and its applications to a spinstand servo system with microactuator. *proceedings of the 9th International Conference on Control, Automation, Robotics and Vision*, pages 1–6, Grant Hyatt, Singapore, 2006.

X. Chen and M. Tomizuka. A minimum parameter adaptive approach for rejecting multiple narrow-band disturbances with application to hard disk drives. *IEEE transactions On Control Systems Technology*, volume 20, number 2, pages 408–415, March, 2012.

M. Mojiri and A. R. Bakhshai. An adaptive notch filter for frequency estimation of a periodic signal. *IEEE transactions On Automatic Control*, volume 49, number 20, pages 314–318, February, 2004.

C. Dai, W. Chen and Y. Zhu Seeker optimization algorithm for digital IIR filter design. *IEEE Transactions On Industrial Electronics*, volume 57, number 5, pages 1710–1718, May, 2010.

J. Levin, N. Prez-Arancibia and P. A. Ioannou. Adaptive Notch Filter Using Real-Time Parameter Estimation *IEEE transactions On Control Systems technology*, Volume 19, number 3, pages 673–681,May, 2011.

X. Guo and M. Bodson Adaptive rejection of disturbance having two sinusoidal components with close and unknown frequencies. *Asian Journal of Control*, volume 14, number 1, pages 36–44, January, 2012.

A. Pyrkin, A. Smyshlyaev, N.B. Liberis and M. Krstic. Rejectionof sinusoidal disturbance of unknown frequency for linear system with input delay. *2010 American Control Conference*, Marriott Waterfront, Baltimore, MD, USA, June 30-July 02, 2010.

S. Pigg and M. Bodson. Adaptive algorithms for the rejection of sinusoidal disturbances acting on unknown plants. *IEEE transactions On Control Systems Technology*, volume 18, number 4, pages 822–836, July, 2010.

S. Aranovskiy, A. Bobtsov, A. Kremle , N. Nikolaev and O. Slita. Identification of frequency of biased harmonic signal. *European Journal of Control*, volume 2, pages 129–139, 2010.

P.A. Regalia. A complex adaptive notch filter. *IEEE signal processing letters*, volume 17, number 11, pages 937–940, November, 2010.

C. C. Took and D. P. Mandic A quaternion widely linear adaptive filter. *IEEE Transactions On Signal Processing*, volume 58, number 8, pages 4427–4431, August, 2010.

M. Ferdjallah and R. E. Barr. Adaptive digital notch filter design on the unit circle for the removal of powerline noise from biomedical signals. *IEEE Transactions On Biomedical Engineering*, volume 41, number 6, pages 529–536, June, 1994.

T. Leng, B. Liu, C. Lu, Z. Zhang and P. Yan. Robust stabilizer design for high-precision tracking of a linear gantry. *Proceedings of the 6th IFAC Symposium on Mechatronic Systems*, Hangzhou, China, pages 362-367, 2013.

J. Doyle, B. Francis and A. Tannenbaum. *feedback control theory*, 1990.